

PAPER • OPEN ACCESS

## Motorbike Vibrations Induced by Surface Irregularities in Road Pavements

To cite this article: M Cavacece 2023 *J. Phys.: Conf. Ser.* **2590** 012005


View the [article online](#) for updates and enhancements.

### You may also like

- [An insight into optical metrology in manufacturing](#)  
Yuki Shimizu, Liang-Chia Chen, Dae Wook Kim et al.
- [A multi-axis MEMS sensor with integrated carbon nanotube-based piezoresistors for nanonewton level force metrology](#)  
Michael A Cullinan, Robert M Panas and Martin L Culpepper
- [Multi-axis control of a qubit in the presence of unknown non-Markovian quantum noise](#)  
Akram Youssry and Hendra I Nurdin

# Motorbike Vibrations Induced by Surface Irregularities in Road Pavements

M Cavacece<sup>1</sup>

<sup>1</sup> University of Cassino and Southern Lazio, Department of Civil and Mechanical Engineering, Via G. Di Biasio, 43 Cassino (FR) Italy 

E-mail: cavacece@unicas.it

**Abstract.** The author proposes a multi-axis equivalent mechanical system with two degrees of freedom on the horizontal plane and five degrees of freedom along the vertical axis to evaluate the accelerations on a motorbike's seat using the state- space representation. The experimental investigations evaluate three types of routes to analyze the comfort vibrational of the motorcycle: paved roads with poor maintenance, road surface with crushed stone, and a road with an artificial bump. Experimental processing considers the gyroscopic and accelerometric signals to deduce the Euler angles. The error analysis evaluates the discrepancy between the accelerations predicted, using the calibrated multi-axis mathematical model, and those obtained in the experimental investigations. The multi-axis model estimates the vibrations on the seat induced by surface irregularities in road pavements. The mathematical prediction obtained by the multi-axis model and experimental investigations analyzes the accelerations in the resonance frequencies of the human spine between 4–12 Hz.

**keywords:** Multi-Axis Mechanical Model, Whole Human Body Vibration, Road Irregularities, Vibrational Comfort

## 1. Introduction

The increasing volume of road traffic, the higher speeds of vehicles, and the increase in axle loads generate vibrations induced by road traffic [1]. The longitudinal irregularity profile represents the deviation at a point along the road [2]. The dynamic response of the motorbikes and the biodynamic response of the human body depend on the road irregularity [3].

The author proposes a multi-axis equivalent mechanical system with two degrees of freedom on the horizontal plane and five degrees of freedom along the vertical axis to evaluate the accelerations on a motorbike's seat using the state- space representation [4]. The experimental investigations evaluate three types of routes to analyze the comfort vibrational of a motorcycle: paved roads with poor maintenance, road surface with crushed stone, and a road with an artificial bump [5]. Experimental investigations by using the motorcycle calibrate the multi-axis equivalent mechanical system [6]. The study implements sensor fusion as a process of fusing data from global position system (GPS), accelerometers, and gyroscopes in such a way as to reduce the measurement uncertainty involved in the navigation movement of the motorbike. The error analysis evaluates the discrepancies between the actual measurements and the simulated measurements of the accelerations and gyro. The purpose of this research is to propose a method to evaluate the vibrations of a motorcycle induced by surface irregularities in road pavements.



## 2. Model of Motorbike for Vibrational Analysis

This research proposes a multi-axis equivalent mechanical system with two degrees of freedom on the horizontal plane and five degrees of freedom along the vertical axis.

### 2.1. Model of Motorbike for Vibrational Analysis on a Horizontal Plane

The model of a motorbike for vibrational analysis on a horizontal plane is subject to the driving force  $F_d$  and two lateral slip forces  $F_r$  and  $F_f$ , applied perpendicular to the corresponding wheels (Fig.1). The non-holonomic constraints act on the center  $G$  of gravity (COG) at  $b$  from  $O$  and  $d$  from  $P$ . The non-holonomic constraints referred to in points  $O$  and  $P$  are the following relations:

$$\begin{aligned} \dot{x}_Q \sin \phi - \dot{y}_Q \cos \phi &= 0 \\ \dot{x}_P \sin (\phi + \psi) - \dot{y}_P \cos (\phi + \psi) &= 0 \end{aligned} \quad (1)$$

the coordinates of the point  $G$  in the world coordinate frame are  $x_G$  and  $y_G$ :

$$\begin{aligned} x_Q &= x_G - b \cos \phi, & x_P &= x_G + d \cos \phi \\ y_Q &= y_G - b \sin \phi, & y_P &= y_G + d \sin \phi \\ \dot{x}_Q &= \dot{x}_G + b\dot{\phi} \sin \phi, & \dot{x}_P &= \dot{x}_G - d\dot{\phi} \sin \phi \\ \dot{y}_Q &= \dot{y}_G - b\dot{\phi} \cos \phi, & \dot{y}_P &= \dot{y}_G + d\dot{\phi} \cos \phi \end{aligned} \quad (2)$$

Introducing the Eq.(1) into Eq.(2) yields

$$\begin{aligned} \dot{x}_G \sin \phi - \dot{y}_G \cos \phi + b\dot{\phi} &= 0 \\ \dot{x}_G \sin (\phi + \psi) - \dot{y}_G \cos (\phi + \psi) - d\dot{\phi} \cos \phi &= 0 \end{aligned} \quad (3)$$

The vector  $[\dot{x}_G, \dot{y}_G]$  indicates the velocity of the COG in the local coordinate frame  $Gx_gy_g$ . The rotational transformation offers the following relation:

$$\begin{Bmatrix} \dot{x}_G \\ \dot{y}_G \end{Bmatrix} = \begin{bmatrix} \cos \phi & -\sin \phi \\ \sin \phi & \cos \phi \end{bmatrix} \begin{Bmatrix} \dot{x}_g \\ \dot{y}_g \end{Bmatrix} \quad (4)$$

Introducing Eq.(3) into Eq.(4) yields:

$$\dot{y}_g = b\dot{\phi}, \quad \dot{\phi} = \frac{\tan \psi}{D} \dot{x}_g \quad (5)$$

The differentiation gives

$$\ddot{y}_g = b\ddot{\phi}, \quad \ddot{\phi} = \frac{\tan \psi}{D} \ddot{x}_g + \frac{1}{D \cos^2 \psi} \dot{x}_g \dot{\psi} \quad (6)$$

by Eq.(5) and Eq.(6)

$$\dot{y}_g = \frac{b}{D} (\tan \psi) \dot{x}_g, \quad \ddot{y}_g = \frac{b}{D} (\tan \psi) \ddot{x}_g + \frac{b}{D \cos^2 \psi} \dot{x}_g \dot{\psi} \quad (7)$$

The Newton-Euler method offers the following dynamic equations:

$$\begin{aligned} m (\ddot{x}_g - \dot{y}_g \dot{\phi}) &= F_d - F_f \sin \psi \\ m (\ddot{y}_g + \dot{x}_g \dot{\phi}) &= F_r + F_f \cos \psi \\ J \ddot{\phi} &= dF_f \cos \psi - bF_r \\ \dot{\psi} &= -\frac{1}{T} \psi + \frac{K_{\text{gain}}}{T} u_s \end{aligned} \quad (8)$$

where  $m$  is the mass;  $J$  the moment of inertia about  $G$ ;  $F_d$  the driving force,  $F_f$ ,  $F_r$  front and rear wheel lateral forces;  $T$  time constant of the steering system;  $u_s$  steering control input;  $K_{\text{gain}}$  a constant coefficient (gain);  $F_d = (1/r)\tau_d$ , with  $r$  the rear wheel radius, and  $\tau_d$  the applied motor torque. The state vector is:

$$\mathbf{x} = [x_G, y_G, \phi, \dot{x}_G, \psi]^T \quad (9)$$

From Eqs.(8)

$$\begin{aligned} m(b\ddot{\phi} + \dot{x}_g\dot{\phi}) &= F_f \cos \psi + \frac{d}{b}F_f \cos \psi - \frac{J}{b}\ddot{\phi} \\ &= \frac{DF_r \cos \psi - J\ddot{\phi}}{b} \quad (D = b + d) \end{aligned} \quad (10)$$

with

$$F_f = \left( \frac{mb^2 + J}{D \cos \psi} \right) + \left( \frac{mb\dot{x}_g}{D \cos \psi} \right) \dot{\phi} \quad (11)$$

The acceleration  $\ddot{x}_g$  becomes

$$\ddot{x}_g = \frac{\dot{x}_g (mb^2 + J)}{a} \dot{\psi} + \frac{D^2 \cos^2 \psi}{a} F_d \quad (12)$$

with

$$a = (\cos^2 \psi) [mD^2 + (mb^2 + J) \tan^2 \psi] \quad (13)$$

The model presents the following relations:

$$\begin{aligned} \dot{x}_G &= \left( \cos \phi - \frac{b}{D} \tan \psi \sin \phi \right) \dot{x}_g \\ \dot{y}_G &= \left( \sin \phi + \frac{b}{D} \tan \psi \cos \phi \right) \dot{x}_g \\ \dot{\phi} &= \left[ \left( \frac{1}{D} \right) \tan \psi \right] \dot{x}_g \\ \ddot{x}_g &= \frac{1}{a} \left[ (mb^2 + J) (\tan \psi) \dot{\psi} \dot{x}_g \right] + \frac{1}{a} (D^2 \cos^2 \psi) F_d \\ \dot{\psi} &= -\frac{1}{T} \psi + \frac{K_{\text{gain}}}{T} u_s \end{aligned} \quad (14)$$

The Eqs.(14) represent a system with two inputs  $(\tau_d, u_s)$ , and a five-dimensional state vector

$$\mathbf{g}_0(x) = \left\{ \begin{array}{c} \left( \cos \phi - \frac{b}{D} \tan \psi \sin \phi \right) \dot{x}_g \\ \left( \sin \phi + \frac{b}{D} \tan \psi \cos \phi \right) \dot{x}_g \\ \left( \frac{1}{D} \right) (\tan \psi) \dot{x}_g \\ \frac{1}{a} \left[ (mb^2 + J) (\tan \psi) \dot{\psi} \dot{x}_g \right] \\ -\frac{1}{T} \psi \end{array} \right\} \quad (15)$$

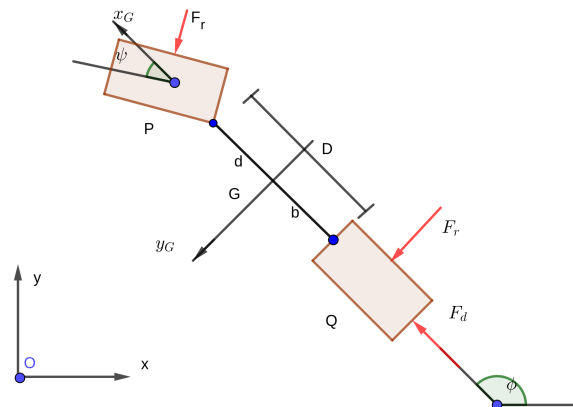


**Figure 1.** Free-body diagram of the equivalent motorbike, eqn. (18):[5]

a drift term:

$$g_1(x) = \left[ 0, 0, 0, 0, \frac{1}{ra} D^2 \cos^2 \psi, 0 \right]^T \quad (16)$$

and the two input fields:

$$g_2(x) = \left[ 0, 0, 0, 0, \frac{K_{gain}}{T} \right]^T \quad (17)$$

or

$$\dot{x}_2 = g_0(x) + g_1(x) \tau_d + g_2(x) u_s \quad (18)$$

## 2.2. Model of Motorbike for Vertical Vibrational Analysis

If the motorcycle runs on the road, the pitch and vertical movements can be represented in the planar vibration model (Fig.2). The motorcycle in its plane of symmetry can be represented as four rigid bodies whose vibrating motion is described by five independent coordinates: the vertical displacement  $z$  of the sprung mass  $m$  center; the pitching rotation  $\theta$  of the sprung mass; the vertical displacement  $z_b$  of mass of driver body  $m_b$ ; the vertical displacements  $z_r$  and  $z_f$  of rear  $m_r$  and front  $m_f$  unsprung mass. The variables  $z$ ,  $z_b$ ,  $\theta$ ,  $z_r$  and  $z_f$  are the general coordinates and time-dependent. The external forces are applied to the front wheel and the rear wheel. The representative mass of the rider's body is  $m_b$ . This mass is connected to the motorcycle by two elements in parallel: a spring element, with elastic constant  $k_b$ , and a damper, with coefficient  $c_b$ . Two degrees of freedom  $z_r$  and  $z_f$  consider the effects of front and rear tire masses in the dynamic model analysis. Two degrees of freedom  $z$  and  $\theta$  consider the effects of the motorcycle frame in the dynamic model analysis.

Lagrange equation proposes the concept of generalized coordinate. Lagrange function offers

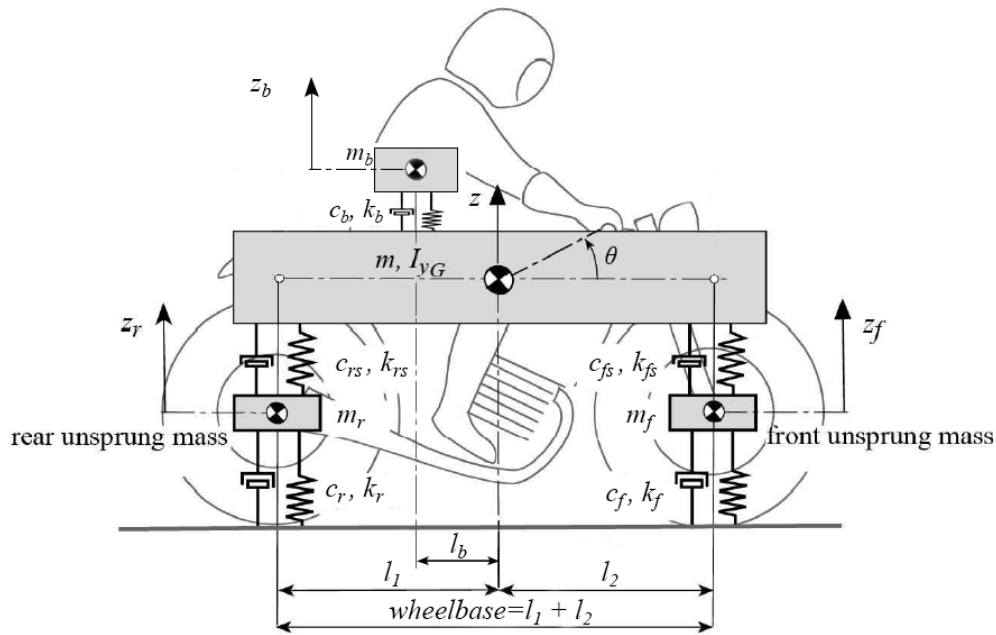


**Figure 2.** Equivalent Mechanical Model of Motorbike for Vibrational Analysis

the following system differential equation of motion:

$$\begin{aligned}
 m\ddot{z} &= k_b(z_b - z) + c_b(\dot{z}_b - \dot{z}) + k_b l_b \theta + c_b l_b \dot{\theta} - k_{fs}(z - z_f) - c_{fs}(\dot{z} - \dot{z}_f) - k_{fs} l_2 \theta \\
 &\quad - c_{fs} l_2 \dot{\theta} - k_{rs}(z - z_r) - c_{rs}(\dot{z} - \dot{z}_r) + k_{rs} l_1 \theta + c_{rs} l_1 \dot{\theta} \\
 I_{yG} \ddot{\theta} &= k_b l_b (z_b - z) + c_b l_b (\dot{z}_b - \dot{z}) - k_b l_b^2 \theta - c_b l_b^2 \dot{\theta} + k_{fs} l_2 (z_f - z) + c_{fs} l_2 (\dot{z}_f - \dot{z}) \\
 &\quad - k_{fs} l_2^2 \theta - c_{fs} l_2^2 \dot{\theta} + k_{rs} l_1 (z_r - z) + c_{rs} l_1 (\dot{z}_r - \dot{z}) - k_{rs} l_1^2 \theta - c_{rs} l_1^2 \dot{\theta} \\
 m_b \ddot{z}_b &= k_b(z - z_b) + c_b(z - z_b) + k_b l_b \theta + c_b l_b \dot{\theta} \\
 m_f \ddot{z}_f &= k_{fs}(z - z_f) + c_{fs}(\dot{z} - \dot{z}_f) + k_{fs} l_2 \theta + c_{fs} l_2 \dot{\theta} - k_f z_f - c_f \dot{z}_f + f_1(t) \\
 m_f \ddot{z}_r &= k_{rs}(z - z_r) + c_{rs}(\dot{z} - \dot{z}_r) + k_{rs} l_1 \theta + c_{rs} l_1 \dot{\theta} - k_r z_r - c_r \dot{z}_r + f_2(t)
 \end{aligned} \tag{19}$$

The matrix representation of the Eq. (19) assumes the following form (Fig. 2)

$$\mathbf{M}\ddot{\mathbf{Z}} + \mathbf{C}\dot{\mathbf{Z}} + \mathbf{K}\mathbf{Z} = \mathbf{F} \tag{20}$$

with the following acceleration, velocity and displacement vectors:

$$\ddot{\mathbf{Z}} = \begin{Bmatrix} \ddot{z} \\ \ddot{\theta} \\ \ddot{z}_b \\ \ddot{z}_f \\ \ddot{z}_r \end{Bmatrix}, \dot{\mathbf{Z}} = \begin{Bmatrix} \dot{z} \\ \dot{\theta} \\ \dot{z}_b \\ \dot{z}_f \\ \dot{z}_r \end{Bmatrix}, \mathbf{Z} = \begin{Bmatrix} z \\ \theta \\ z_b \\ z_f \\ z_r \end{Bmatrix}, \tag{21}$$

the external force vector  $\mathbf{F}$ , the mass matrix  $\mathbf{M}$ , the damping matrix  $\mathbf{C}$  and the stiffness matrix

**K** are the following expressions:

$$\mathbf{F} = \begin{Bmatrix} 0 \\ 0 \\ 0 \\ f_1 \\ f_2 \end{Bmatrix}, \quad \mathbf{M} = \begin{bmatrix} m & 0 & 0 & 0 & 0 \\ 0 & I_{yG} & 0 & 0 & 0 \\ 0 & 0 & m_b & 0 & 0 \\ 0 & 0 & 0 & m_f & 0 \\ 0 & 0 & 0 & 0 & m_r \end{bmatrix},$$

$$\mathbf{C} = \begin{bmatrix} (c_{rs} + c_{fs} + c_b) & (c_{fs}l_2 - c_{rs}l_1 + c_b l_b) & -c_b & -c_{fs} & -c_{rs} \\ (c_{fs}l_2 - c_{rs}l_1 + c_b l_b) & (c_{rs}l_1^2 + c_{fs}l_2^2 + c_b l_b^2) & -c_b l_b & -c_{fs}l_2 & -c_{rs}l_1 \\ -c_b & -c_b l_b & c_b & 0 & 0 \\ -c_{fs} & -c_{fs}l_2 & 0 & (c_{fs} + c_f) & 0 \\ -c_{rs} & -c_{rs}l_1 & 0 & 0 & (c_{rs} + c_r) \end{bmatrix},$$

$$\mathbf{K} = \begin{bmatrix} (k_{rs} + k_{fs} + k_b) & (k_{fs}l_2 - k_{rs}l_1 + k_b l_b) & -k_b & -k_{fs} & -k_{rs} \\ (k_{fs}l_2 - k_{rs}l_1 + k_b l_b) & (k_{rs}l_1^2 + k_{fs}l_2^2 + k_b l_b^2) & -k_b l_b & -k_{fs}l_2 & -k_{rs}l_1 \\ -k_b & -k_b l_b & k_b & 0 & 0 \\ -k_{fs} & -k_{fs}l_2 & 0 & (k_{fs} + k_f) & 0 \\ -k_{rs} & -k_{rs}l_1 & 0 & 0 & (k_{rs} + k_r) \end{bmatrix}. \quad (22)$$

The State–Space representation proposes the dynamical analysis of the equivalent mechanical model of motorbike along vertical axis. The second–order differential equations of motion represents the physical system as a set of state variables, input vectors and output vector related to system of first–order differential equations. The Eq. (20) is rewritten in the following equivalent sistem:

$$\begin{cases} \mathbf{M}\ddot{\mathbf{Z}} = -\mathbf{C}\dot{\mathbf{Z}} - \mathbf{K}\mathbf{Z} + \mathbf{F} \\ \mathbf{M}\dot{\mathbf{Z}} = \mathbf{M}\dot{\mathbf{Z}} \iff \dot{\mathbf{Z}} = \dot{\mathbf{Z}} \end{cases} \quad (23)$$

or in matrix form

$$\begin{bmatrix} \mathbf{M} & \mathbf{0} \\ \mathbf{0} & \mathbf{M} \end{bmatrix} \begin{Bmatrix} \ddot{\mathbf{Z}} \\ \dot{\mathbf{Z}} \end{Bmatrix} = \begin{bmatrix} -\mathbf{C} & -\mathbf{K} \\ \mathbf{M} & \mathbf{0} \end{bmatrix} \begin{Bmatrix} \dot{\mathbf{Z}} \\ \mathbf{Z} \end{Bmatrix} + \begin{Bmatrix} \mathbf{F} \\ \mathbf{0} \end{Bmatrix} \quad (24)$$

$$\begin{Bmatrix} \ddot{\mathbf{Z}} \\ \dot{\mathbf{Z}} \end{Bmatrix} = \begin{bmatrix} \mathbf{M} & \mathbf{0} \\ \mathbf{0} & \mathbf{M} \end{bmatrix}^{-1} \begin{bmatrix} -\mathbf{C} & -\mathbf{K} \\ \mathbf{M} & \mathbf{0} \end{bmatrix} \begin{Bmatrix} \dot{\mathbf{Z}} \\ \mathbf{Z} \end{Bmatrix} + \begin{bmatrix} \mathbf{M} & \mathbf{0} \\ \mathbf{0} & \mathbf{M} \end{bmatrix}^{-1} \begin{Bmatrix} \mathbf{F} \\ \mathbf{0} \end{Bmatrix}.$$

The Eq. (24) offers the Motorcycle model in spaces of states time invariant in its continuous form:

$$\begin{cases} \dot{X} = AX + BF \\ Y = EX + DF \end{cases} \quad (25)$$

The output vector  $Y$  and the state vector  $X$  provide the following relation:

$$Y^T = X^T = \{\dot{\mathbf{Z}} \quad \mathbf{Z}\}^T, \quad (26)$$

the state matrix  $A$ :

$$A = \begin{bmatrix} \mathbf{M} & \mathbf{0} \\ \mathbf{0} & \mathbf{M} \end{bmatrix}^{-1} \begin{bmatrix} -\mathbf{C} & -\mathbf{K} \\ \mathbf{M} & \mathbf{0} \end{bmatrix}, \quad (27)$$

with the matrix  $B' = BF$ , where  $B$  is the input matrix

$$B = \begin{bmatrix} \mathbf{M} & \mathbf{0} \\ \mathbf{0} & \mathbf{M} \end{bmatrix}^{-1} \begin{bmatrix} 0 & 0 \\ 0 & 0 \\ 0 & 0 \\ 1 & 0 \\ 0 & 1 \\ 0 & 0 \\ 0 & 0 \\ \vdots & \vdots \\ 0 & 0 \end{bmatrix}, \quad (28)$$

and  $\mathcal{F}$  the input vector

$$\mathcal{F} = \begin{Bmatrix} f_1(t) \\ f_2(t) \end{Bmatrix}, \quad (29)$$

The output matrix  $E$  and the direct transition matrix or feedthrough  $D$  are

$$E = \begin{bmatrix} 0 & 0 & 0 & 0 & 0 & 1 & 0 & 0 & 0 & 0 \\ 0 & 0 & 0 & 0 & 0 & 0 & 1 & 0 & 0 & 0 \\ 0 & 0 & 0 & 0 & 0 & 0 & 0 & 1 & 0 & 0 \\ 0 & 0 & 0 & 0 & 0 & 0 & 0 & 0 & 1 & 0 \\ 0 & 0 & 0 & 0 & 0 & 0 & 0 & 0 & 0 & 1 \end{bmatrix} \quad \text{and} \quad D = \begin{bmatrix} 0 & 0 & 0 & 0 & 0 \\ 0 & 0 & 0 & 0 & 0 \\ 0 & 0 & 0 & 0 & 0 \\ 0 & 0 & 0 & 0 & 0 \\ 0 & 0 & 0 & 0 & 0 \end{bmatrix}. \quad (30)$$

The system of equations (25) offers discrete time equivalent to analyze the behavior of the model as a function of a discrete input:

$$\begin{cases} \dot{X}(k+1) = \mathbf{A}_d X(k) + \mathbf{B}_d U(k) \\ Y(k) = \mathbf{E}X(k) + \mathbf{D}U(k) \end{cases} \quad (31)$$

where  $\mathbf{A}_d$  and  $\mathbf{B}_d$  are the discrete matrices of state with input matrix  $\mathbf{A}$  and  $\mathbf{B}$ :

$$\mathbf{A}_d = e^{\mathbf{A}\Delta t} \quad \text{and} \quad \mathbf{B}_d = \mathbf{A}^{-1}(\mathbf{A}_d - \mathbf{I})\mathbf{B}. \quad (32)$$

The vector  $U$  is the discrete input vector, similar to  $\mathcal{F}$ , with components  $u_1(k)$  and  $u_2(k)$  for the front and rear tires:

$$U = \begin{Bmatrix} u_1(k) \\ u_2(k) \end{Bmatrix}. \quad (33)$$

The Eq. (31) predicts the stresses acting on the wheels of the motorbike caused by the road profile. The state space model provides the prediction of acceleration values in function of the road profile in the time domain.

### 3. Strapdown Attitude Propagation

Experimental processing considers the gyroscopic and accelerometric signal to deduce the direct cosine matrix (Fig.3). If the motion frequency is close to or higher than the sampling frequency, attitude integration considers the time-dependent attitude trajectory called coning motion (Fig.4). It is assumed that the attitude trajectory takes the following expression:

$$\rho(t) = \theta_{cone} \begin{Bmatrix} \cos(\Omega_{coning}t) \\ \sin(\Omega_{coning}t) \\ 0 \end{Bmatrix}, \quad (34)$$



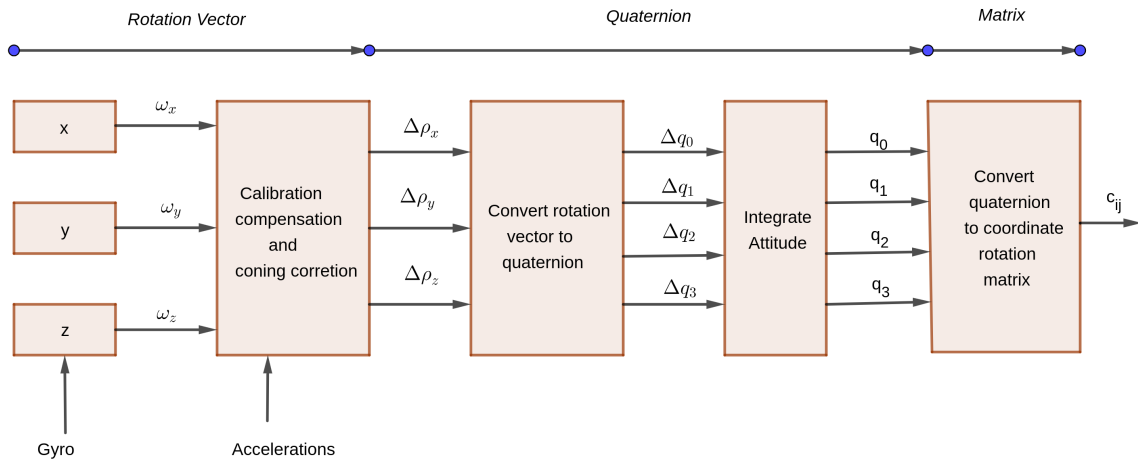


**Figure 3.** Strapdown attitude representations, eqn. (38):[6]

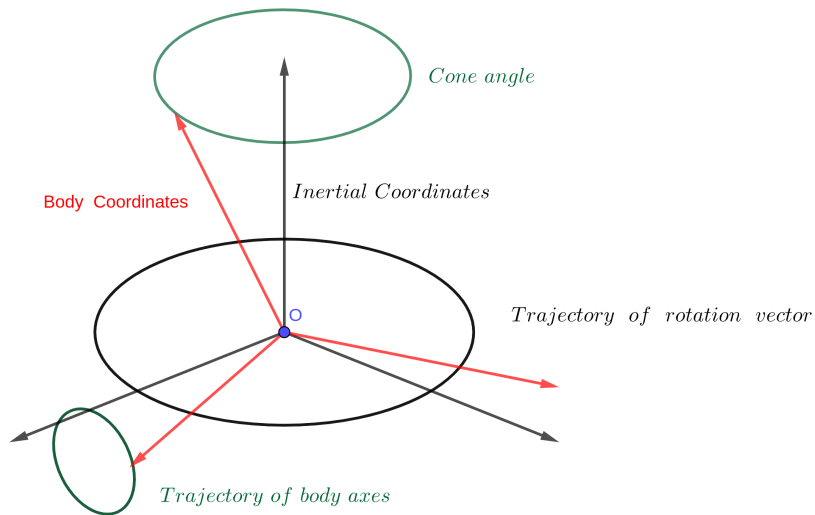


**Figure 4.** Coning motion, eqn. (34):[5]

where  $\rho$  is the rotation vector;  $\theta_{cone}$  is called the cone angle of the motion;  $\Omega_{coning}$  is the coning frequency of the motion. The derivative of the rotation vector is

$$\dot{\rho}(t) = \theta_{cone} \cdot \Omega_{coning} \begin{Bmatrix} -\sin(\Omega_{coning}t) \\ \cos(\Omega_{coning}t) \\ 0 \end{Bmatrix}, \quad (35)$$

The coordinate transformation matrix from body coordinates to inertial coordinates offers

the following relation

$$\begin{aligned} C_{inertial}^{body} &= \cos \theta I + (1 - \cos \theta) \\ &= \begin{bmatrix} \cos(\Omega_{coning} t)^2 & \sin(\Omega_{coning} t) \cos(\Omega_{coning} t) & 0 \\ \sin(\Omega_{coning} t) \cos(\Omega_{coning} t) & \sin(\Omega_{coning} t)^2 & 0 \end{bmatrix} \\ &+ \sin \theta \begin{bmatrix} 0 & 0 & \sin(\Omega_{coning} t) \\ 0 & 0 & -\cos(\Omega_{coning} t) \\ -\sin(\Omega_{coning} t) \cos(\Omega_{coning} t) & 0 & 0 \end{bmatrix}, \end{aligned} \quad (36)$$

the measured inertial rotation rates in body coordinates is the following relation

$$\begin{aligned} \omega_{body} &= C_{inertial}^{body} \dot{\rho}_{inertial} = \theta_{coning} \Omega_{coning} \left\{ C_{inertial}^{body} \right\}^T \begin{Bmatrix} -\sin(\Omega_{coning} t) \\ \cos(\Omega_{coning} t) \\ 0 \end{Bmatrix}, \\ &= \begin{Bmatrix} -\theta_{coning} \Omega_{coning} \sin(\Omega_{coning} t) \cos(\theta_{coning}) \\ \theta_{coning} \Omega_{coning} \cos(\Omega_{coning} t) \cos(\theta_{coning}) \\ -\theta_{coning} \Omega_{coning} \sin(\theta_{coning}) \end{Bmatrix}, \end{aligned} \quad (37)$$

The rate integrating gyroscope is

$$\int_{s=0}^t \omega_{body}(s) ds = \begin{Bmatrix} -\theta_{coning} \cos(\theta_{coning}) [1 - \cos(\Omega_{coning} t)] \\ \theta_{coning} \cos(\theta_{coning}) \sin(\Omega_{coning} t) \\ -\sin(\theta_{coning}) \theta_{coning} \Omega_{coning} t \end{Bmatrix}, \quad (38)$$

John Bortz developed the exact model for attitude integration based on measured rotation rates and rotation vectors:

$$\dot{\rho} = \omega + f_{Bortz}(\omega, \rho) \quad (39)$$

where  $\omega$  is the vector of measured rotation rates. The Bortz *noncommutative rate vector* becomes the following relation

$$f_{Bortz}(\omega, \rho) = \frac{1}{2} \rho \otimes \omega + \frac{1}{\rho} \left\{ 1 - \frac{\|\rho\| \sin(\|\rho\|)}{2[1 - \cos(\|\rho\|)]} \right\} \rho \otimes (\rho \otimes \omega) \quad |\rho| < \frac{\pi}{2} \quad (40)$$

The rotation vector represents the change in body attitude

$$\delta \rho = \int_0^{\delta t} \dot{\rho}[\rho(s) + \omega(s)] ds, \quad (41)$$

The successive step transforms the incremental rotations into incremental quaternions. The implementation of the Bortz conoid correction gives the following incremental rotation vector  $\delta \rho$  from which the equivalent incremental quaternion  $\Delta q$  takes on the following expression:

$$\theta = |\Delta \rho|, \quad u = \frac{1}{\theta} \Delta \rho = \begin{Bmatrix} u_1 \\ u_2 \\ u_3 \end{Bmatrix}, \quad \Delta q = \begin{Bmatrix} \cos \frac{\theta}{2} \\ u_1 \sin \frac{\theta}{2} \\ u_2 \sin \frac{\theta}{2} \\ u_3 \sin \frac{\theta}{2} \end{Bmatrix} = \begin{Bmatrix} \delta q_0 \\ \delta q_1 \\ \delta q_2 \\ \delta q_3 \end{Bmatrix}, \quad (42)$$

The update equation for quaternion representation of attitude is the following relation:

$$q_k = \Delta q \times q_{k-1} \times \delta q^* \quad q_{inertial}^{body} = \begin{Bmatrix} \delta q_0 \\ \delta q_1 \\ \delta q_2 \\ \delta q_3 \end{Bmatrix} \quad (43)$$

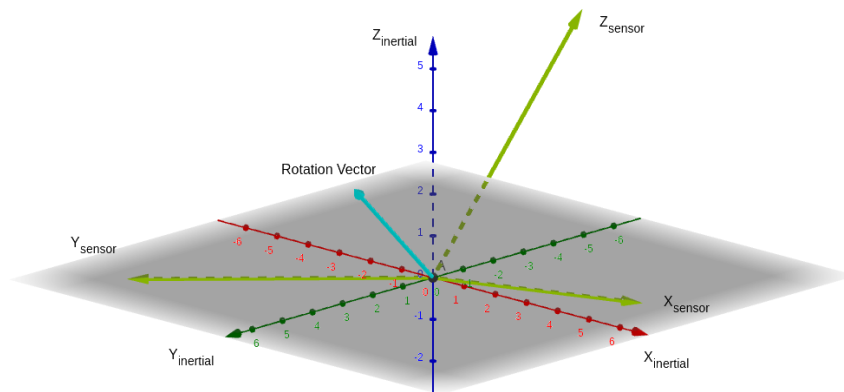


**Figure 5.** Representing Coordinate Transformation by Rotation Vector, eqn. (44):[5]

where the quaternion  $q_{k-1}$  represents the prior value of attitude, the quaternion  $\Delta q$  is the change in attitude, and the quaternion  $q_k$  represents the updated value of attitude. The symbol  $(\times)$  defines the quaternion multiplication and the superscript  $(*)$  represents the conjugate of a quaternion. The coordinate transformation matrix  $C_{inertial}^{body}$  from fixed body coordinates to inertial coordinates transforms measured changes in velocity into inertial coordinates (Fig.5). The quaternion representation offers the direction cosines matrix  $C_{inertial}^{body}$  from body-fixed coordinates to inertial coordinates:

$$C_{inertial}^{body} = (2q_0^2 - 1) I_3 + 2 \begin{Bmatrix} \delta q_1 \\ \delta q_2 \\ \delta q_3 \end{Bmatrix} \times \begin{Bmatrix} \delta q_0 \\ \delta q_1 \\ \delta q_2 \\ \delta q_3 \end{Bmatrix}^T - 2q_0 \begin{Bmatrix} \delta q_1 \\ \delta q_2 \\ \delta q_3 \end{Bmatrix} \begin{bmatrix} (2q_0 - 1 + q_1^2) & (2q_1q_2 + 2q_0q_3) & (2q_1q_3 - 2q_0q_2) \\ (2q_1q_2 - 2q_0q_3) & (2q_0^2 - 1 + 2q_2^2) & (2q_2^2 + 2q_0q_1) \\ (2q_1q_3 + 2q_0q_2) & (2q_2^2 - 2q_0q_1) & (2q_0^2 - 1 + 2q_3^2) \end{bmatrix} \quad (44)$$

#### 4. Error Analysis by Relative Localization

Relative tracking measures the movement of the motorbike between two assigned positions on a smooth road profile. The measurements estimate the average distance traveled from the starting position if the motorbike moves. The analysis of the time and frequency domains frequency domain allows the calibration of the multi-axis mathematical model of the motorbike.

Wheel slip can generate non-systematic measurement errors caused by slippery floors, excessive accelerations, non-point contact with the floor, and skidding. The discrepancy between the accelerations predicted using the calibrated multi-axis mathematical model and those deduced in the experimental investigations offers the assessment of non-systematic errors (Fig.6).

#### 5. Experimental Setup

The driving comfort has been studied using a touring motorcycle with total length of 2126 mm, a width of 850 mm, a height 1430 mm, a wheelbase 1500 mm, and a weight 215 Kg (Figures

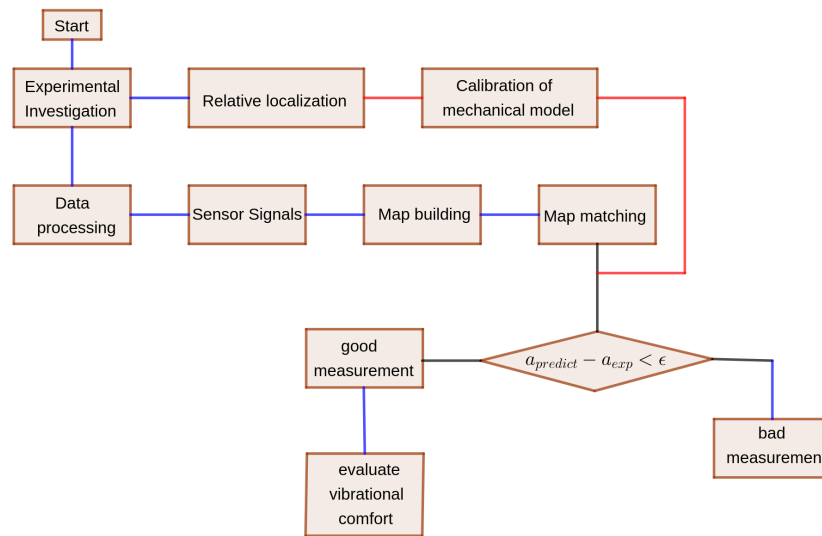


**Figure 6.** Structure of map based localization, eqn. (25):[5]

1– 2). Seat Accelerometer SV38V is positioned on the seat of the motorbike. The experimental investigations have analyzed the conditions of comfort in the following cases: roads with poor maintenance, roads with stone pavement, and roads with artificial bumps. The experimental investigations include five tests of 5 minutes on-road profiles with poor asphalt maintenance, and five tests of 5 minutes on cobblestones road, and five tests of one minute on the bumpy road. The speed of the motorbike is about 50 km/h.

## 6. Discussion

The bumpy road causes impulsive input stresses, reaching high acceleration values of 115 m/s<sup>2</sup> as peak, corresponding to about 10 g in a short time along vertical axis. The response to this stress is caused by crossing the bumpy road. The MIMO model identifies the following three peaks: 1.6–2 Hz, 12.5 Hz, and 50 Hz along vertical axis. The maximum peak is at about 12.5 Hz. The third resonant frequency of human spine is 12.70 Hz. (Fig.7).

The second type of route considers a profile road with irregular stones. The loads acting on the motorcycle are very high. The rider perceives the highest stress values. The mathematical model and experimental investigations show peaks at 1.6 Hz, 12.5 Hz, and 50 Hz along vertical axis. The first, second and third resonance frequencies of the human spine are stressed (Fig.8). The experimental investigations on road surface with poor asphalt maintenance and represented in frequency domain propose an acceleration evaluated on the seat (Fig.9). Frequency analysis of acceleration evaluated on the seat offer three peaks of vibration at 1.6 Hz, 12.5 Hz, and 50 Hz with low acceleration values in the frequency range 4–12.50 Hz (Fig.9).

## 7. Conclusion

The mathematical prediction and experimental investigations show that the resonance frequencies of the spine between 4–12 Hz are not stressed with poor asphalt maintenance and on cobblestones road. The motorbike offers excellent conditions of vibrational comfort on the bumpy road, allowing the rider a satisfactory driving experience even in disadvantageous conditions and road profiles.

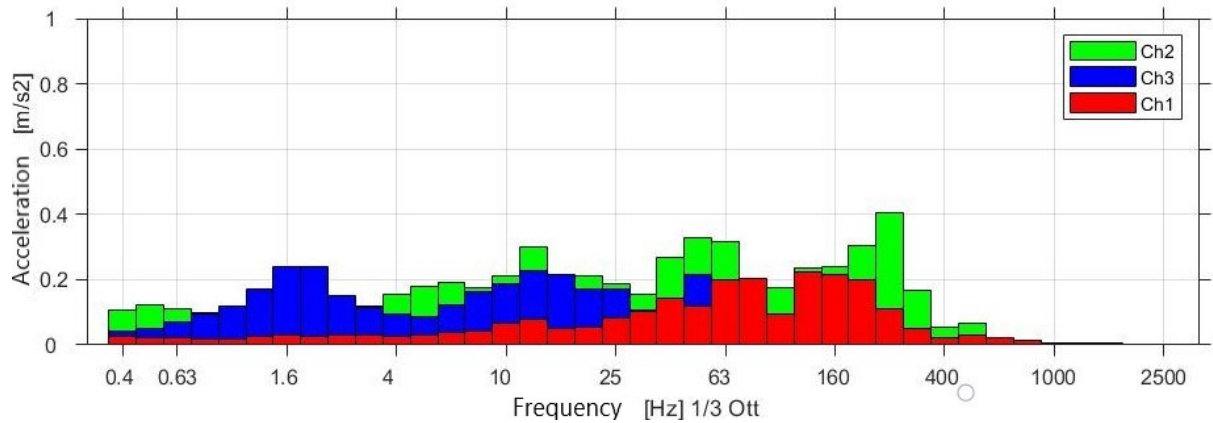


**Figure 7.** Acceleration on the seat caused by bumpy road and represented in frequency domain

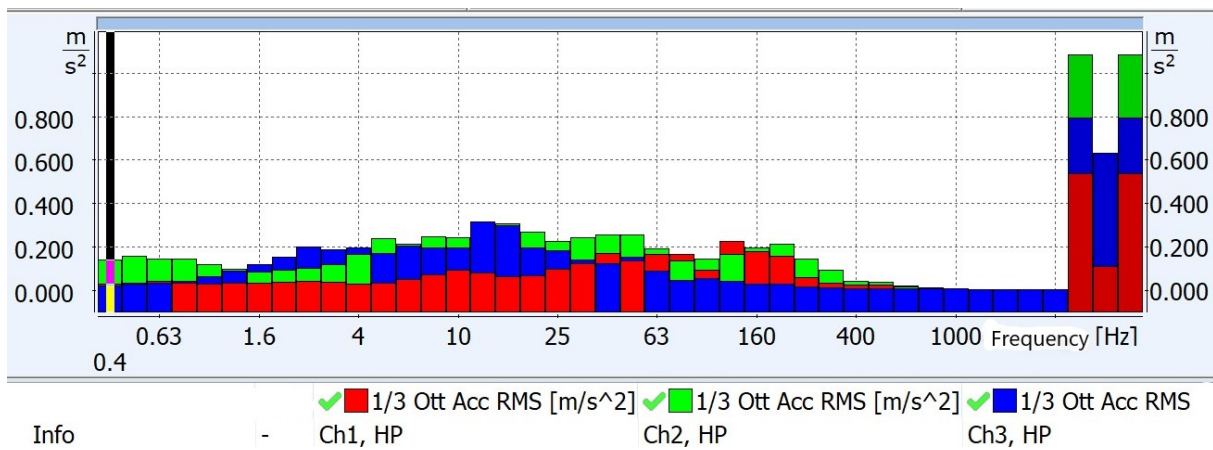


**Figure 8.** Acceleration on the seat caused by cobblestones road and represented in frequency domain

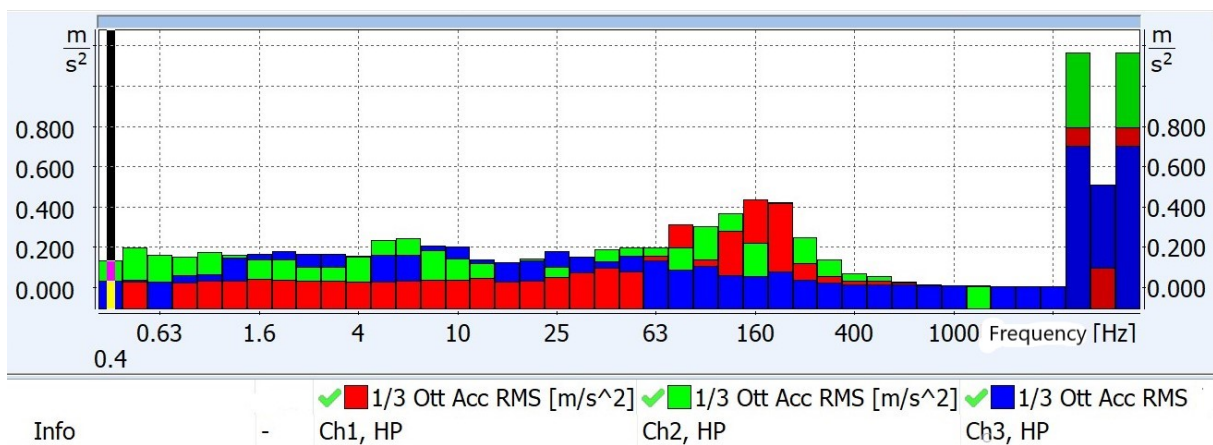


**Figure 9.** Acceleration on the seat caused by road surface with poor asphalt maintenance and represented in frequency domain

## References

- [1] Cossalter V., Da Lio M., Lot R., Fabbri L., A General Method for the Evaluation of Vehicle Manoeuvrability with Special Emphasis on Motorcycles, Vehicle System Dynamics, 31, 2, 1999, pp.113–

**Table 1.** Nomenclature

---

$m$	equivalent mass of the motor vehicle
$m_b$	equivalent mass of the human body
$m_f$	mass of the front wheel
$m_r$	mass of the rear wheel
$I_{yG}$	motorcycle moment of inertia
$c_{fs}$	viscous damping of the front suspension
$k_{fs}$	stiffness of the front suspension
$z_b$	coordinate related to the human body of the driver
$c_{rs}$	viscous damping of the rear suspension
$k_{rs}$	stiffness of the rear suspension
$c_f$	viscous damping of the front tyre
$k_f$	stiffness of the front tyre
$c_r$	viscous damping of the rear tyre
$k_r$	stiffness of the rear tyre
$\theta$	coordinate of the motorcycle
$z$	coordinate of the motorcycle
$z_r$	rear tyre coordinate
$z_f$	front tyre coordinate

---

135, 10.1076/vesd.31.2.113.2094.

- [2] Cossalter V, Motorcycle Dynamics, Lulu.com, 2002.
- [3] Cossalter V., Lot R., A motorcycle multi-body model for real time simulations based on the natural coordinates approach, Vehicle system dynamics, 37, 6, 2002, pp. 423-447.
- [4] Cossalter V., Lot R., Massaro M., Discussion on: Experimental Identification of the Engine-to-Slip Dynamics for Traction Control Applications in a Sport Motorcycle, European Journal of Control, 16, 1, 2010, pp.113-114, ISSN 0947-3580, [https://doi.org/10.1016/S0947-3580\(10\)70628-2](https://doi.org/10.1016/S0947-3580(10)70628-2).
- [5] Cavacece M., Figliolini G., Lanni C., Vertical Vibrations of the Vehicle Excited by Ride Test. In: Rao Y.V.D., Amarnath C., Regalla S.P., Javed A., Singh K.K. (eds) Advances in Industrial Machines and Mechanisms. Lecture Notes in Mechanical Engineering. Springer, Singapore, 2021, 631-642, <https://doi.org/10.1007/978-981-16-1769-0-57>.
- [6] Cavacece M, Comfort Assessment in Railway Vehicles by an Optimal Identification of Transfer Function, Universal Journal of Mechanical Engineering, Vol. 10, No. 1, pp. 1-12, 2022, 10.13189/ujme.2022.100101.